Determination and Quantification of the Local Environments in Stoichiometric and Defect Jarosite by Solid-State ^{2}H NMR Spectroscopy

Ulla Gro Nielsen,[†,‡] Juraj Majzlan,[§] and Clare P. Grey*[,†]

Department of Chemistry and Center for Environmental Molecular Sciences, Stony Brook University, Stony Brook, New York 11794-3400, and Institute for Mineralogy and Geochemistry, Albert-Ludwig University of Freiburg, Albertstrasse 23b, Freiburg D-79104, Germany

Received September 4, 2007. Revised Manuscript Received November 8, 2007

The nature and concentrations of the local environments in a series of deuterated jarosite (nominally $AFe_3(SO_4)_2(OD)_6$ with A = K, Na, and D_3O) samples with different levels of iron and cation vacancies have been determined by ^{2}H MAS NMR spectroscopy at ambient temperatures. Three different local deuteron environments, Fe_2OD, $FeOD_2$, and D_2O/D_3O^+, can be separated based on their very different Fermi contact shifts of $\delta \approx 237$, 70, and 0 ppm, respectively. The $FeOD_2$ group arises from the charge compensation of the Fe^{3+} vacancies, allowing the concentrations of the vacancies to be readily determined. Analysis of the ^{2}H quadrupole interaction indicates that the $FeOD_2$ groups are mobile, undergoing rapid 180° flips on the NMR time scale; the D_2O/D_3O^+ species (located on the A sites) undergo close to isotropic motion, whereas the Fe_2OD groups are rigid and are hydrogen-bonded to nearby sulfate O atoms, with a (Fe)OD−O(S) distance of 2.79(4) Å. No evidence for the intrinsic protonation reaction $Fe_2OH + H_3O^+ \rightarrow Fe_2OH_2 + H_2O$ is found in the hydronium jarosite, suggesting that this mechanism is not the cause of the anomalous magnetic behavior of this material. The results illustrate that ^{2}H MAS NMR spectroscopy is an excellent probe of the local environments and defects, on the atomic/molecular level, providing information that is complementary to diffraction techniques and that will help to rationalize the magnetic properties of these materials.

Introduction

Mixed-metal iron hydroxysulfates with the general formula $AFe_3(SO_4)_2(OH)_6$ (A = H_3O, Na, K, Rb, and $^1/_2$Pb, etc.) belong to the jarosite group of minerals.[1] They occur in nature, where they are generally formed in the acidic aqueous environments that are often associated with acid mine drainage sites.[2] The jarosite group of minerals can act as sinks for toxic ions such as arsenate, chromate, thallium, lead, and cadmium.[1,3,4] In addition, the observation of jarosite on Mars served as evidence for the presence of water in the geological past of the planet's surface.[5–7] Jarosite has been extensively studied as a textbook example of a frustrated Kagomé−Heisenberg antiferromagnet.[8–18] The magnetic properties, especially the observation of long-range order in most jarosite samples, except for the spin-glass hydronium jarosite, are currently receiving much attention, with the debate especially centering on the role played by the defects and hydronium ions in controlling magnetic ordering.[9–11,13,16–26]

* Corresponding author. Fax: 1-631-632-5731. E-mail: cgrey@notes.cc.sunysb.edu.
† Stony Brook University.
‡ Current address: Department of Physics and Chemistry, University of Southern Denmark, Campusvej 55, 5230 Odense M, Denmark.
§ Albert-Ludwig University of Freiburg.

(1) Stoffregen, R. E.; Alpers, C. N.; Jambor, J. L. Alunite-jarosite crystallography, thermodynamics, and geochronology. In *Sulfate Minerals—Crystallography, Geochemistry and Environmental Significance*; Alpers, C. N., Jambor, J. L., Nordstrom, D. K., Eds.; Mineralogical Society of America: Washington, DC. Eds.
(2) Alpers, C. N.; Rye, R. O.; Nordstrom, D. K.; White, L. D.; King, B. S. *Chem. Geol.* **1992**, *96*, 203.
(3) Baron, D.; Palmer, C. D. *Geochim. Cosmochim. Acta* **1996**, *60*, 3815.
(4) Savage, K. S.; Bird, D. K.; O'Day, P. A. *Chem. Geol.* **2005**, *215*, 473.
(5) Klingelhöfer, G.; et al. *Science* **2004**, *306* (5702), 1740–1745.
(6) Madden, M. E. E.; Bodnar, R. J.; Rimstidt, J. D. *Nature* **2004**, *431*, 821.
(7) Squyres, S. W.; et al. *Science* **2004**, *306*, 1709.
(8) Townsend, M. G.; Longworth, G.; Roudaut, E. *Phys. Rev. B* **1986**, *33*, 4919.
(9) Wills, A. S.; Harrison, A. *J. Chem. Soc., Faraday Trans.* **1996**, *92*, 2161.
(10) Harrison, A.; Wills, A. S.; Ritter, C. *Physica B* **1998**, *241*, 722.
(11) Wills, A. S.; Harrison, A.; Ritter, C.; Smith, R. I. *Phys. Rev. B* **2000**, *61*, 6156.
(12) Greedan, J. E. *J. Mater.Chem.* **2001**, *11*, 37.
(13) Grohol, D.; Nocera, D. G.; Papoutsakis, D. *Phys. Rev. B* **2003**, *67*, 064401.
(14) Nishiyama, M.; Maegawa, S.; Inami, T.; Oka, Y. *Phys. Rev. B* **2003**, *67*, 224435.
(15) Nocera, D. G.; Bartlett, B. M.; Grohol, D.; Papoutsakis, D.; Shores, M. P. *Chem.—Eur. J.* **2004**, *10*, 3851.
(16) Grohol, D.; Matan, K.; Cho, J. H.; Lee, S. H.; Lynn, J. W.; Nocera, D. G.; Lee, Y. S. *Nat. Mater.* **2005**, *4*, 323.
(17) Matan, K.; Grohol, D.; Nocera, D. G.; Yildirim, T.; Harris, A. B.; Lee, S. H.; Nagler, S. E.; Lee, Y. S. *Phys. Rev. Lett.* **2006**, *96*, 247201.
(18) Yildirim, T.; Harris, A. B. *Phys. Rev. B* **2006**, *73*, 214446.
(19) Bartlett, B. M.; Nocera, D. G. *J. Am. Chem. Soc.* **2005**, *127*, 8985.
(20) Majzlan, J.; Stevens, R.; Boerio-Goates, J.; Woodfield, B. F.; Navrotsky, A.; Burns, P. C.; Crawford, M. K.; Amos, T. G. *Phys. Chem. Miner.* **2004**, *31*, 518.
(21) Harrison, A.; Kojima, K. M.; Wills, A. S.; Fudamato, Y.; Larkin, M. I.; Luke, G. M.; Nachumi, B.; Uemura, Y. J.; Visser, D.; Lord, J. S. *Physica B* **2000**, *217*, 289–290.
(22) Harrison, A. *J. Phys.: Condens. Matter* **2004**, *16*, S553.
(23) Inami, T.; Maegawa, S.; Takano, M. *J. Magn. Magn. Mater.* **1998**, *752*, 177–181.
(24) Nishiyama, M.; Maegawa, S. *Physica B* **2003**, *1065*, 329–333.

10.1021/cm702523d CCC: $40.75
Published on Web 02/29/2008

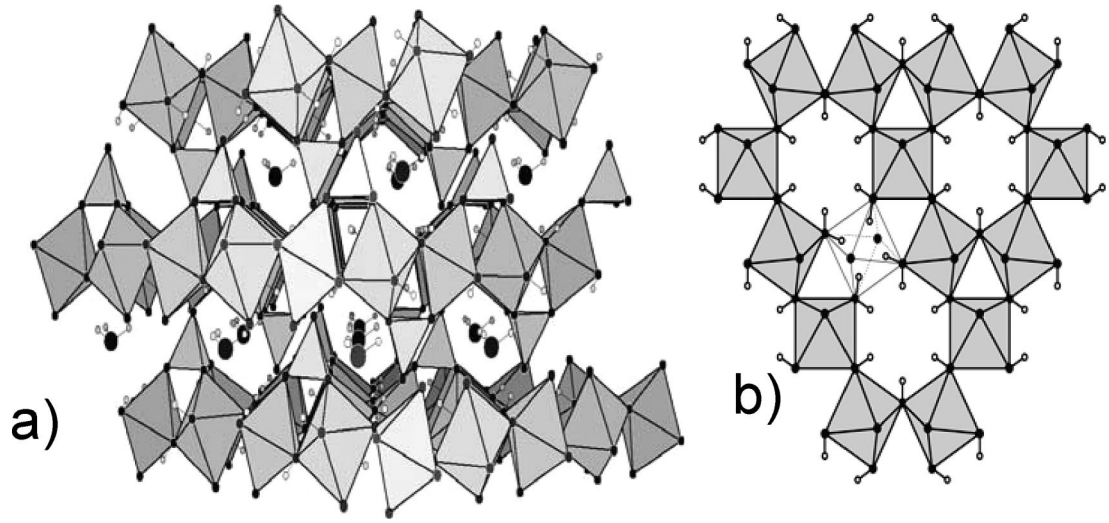

Figure 1. (a) Structure of hydronium jarosite, viewed along the [001] direction showing the Fe^{3+} octahedra and the SO_4^{2-} tetrahedra. The monovalent hydronium ions are located between the Fe^{3+} octahedral sheets in large cavities. (b) The local environment near an Fe^{3+} vacancy.

The structure of jarosite (Figure 1) consists of sheets of octahedrally coordinated iron(III) cations. The iron(III) ions are located on a triangular, so-called Kagomé lattice, and it is this arrangement that is responsible for the magnetic frustration of jarosite. Three iron cations at the corners of an equilateral triangle form the magnetic subunit and cause the spin frustration. Each iron(III) ion forms four equatorial O(H) bonds and two axial bonds to oxygen atoms from two sulfate groups. The monovalent cations are located in cavities between the octahedral sheets and are coordinated by 12 oxygen atoms or hydroxyl groups. There is a weak hydrogen bond between the bridging hydroxyl group and the apical oxygen atom of the sulfate group with a O−O distance of ca. 2.82 Å.[9]

Naturally occurring and synthetic jarosite samples often have high concentrations (10–30%) of Fe^{3+} and A vacancies.[9,12] These defects alter the magnetic properties, as illustrated by a decrease in the Néel temperature (T_N) to below the 61–65 K value typical of stoichiometric samples, and a reduction in the average magnetic moments above T_N.[1,9,11–13,15,19,20,26,27] The observation of long-range order in jarosite samples was originally ascribed to the presence of iron vacancies.[9,11] However, long-range magnetic order is observed even in the stoichiometric, large single-crystal jarosite samples prepared by the synthesis method of Grohol et al.[13,16,28] As a consequence of these observations, long-range magnetic order is assigned to the dipolar coupling (Dzyaloshinskii−Moriya) interaction caused by the tilting of the iron octahedra and thus the formation of nonparallel spins ($S_i \times S_j \neq 0$).[15–18,29]

Hydronium jarosite is the only compound that does not exhibit long-range magnetic order but is a spin glass instead with a glass transition temperature of around 15 K.[9,10,20] This lack of long-range magnetic order has been ascribed by Grohol et al. to a combination of an intrinsic protonation reaction involving the Fe_2OH bridging OH groups, $Fe_2OH + H_3O^+ \rightarrow Fe_2OH_2 + H_2O$, and the disorder of the hydrogen atoms of the H_2O/H_3O^+ groups in the structure.[13,26] This deprotonation reaction was proposed in this system based on their infrared (IR) spectra and susceptibility data.[13,26] In contrast to this, our recent multinuclear NMR study of isostructural alunite samples ($AAl(SO_4(OH)_6$) demonstrated that the hydronium ion is present only in stoichiometric regions of the alunite samples but is deprotonated in regions containing Al^{3+} vacancies, □, i.e.

$$M(OH)_4O_2 + 3H^+ + H_3O^+ \rightarrow \square^+(OH_2)_4O_2 + H_2O + M^{3+} \quad (1)$$

a model that is also consistent with the elemental analysis.[30]

In contrast to NMR, most other techniques commonly employed in studies of jarosite have provided insight to the average properties of the sample such as magnetic susceptibility, chemical composition, and crystal structure. However, information about proton speciation and mobility is very difficult to obtain directly with these methods. For example, diffraction provides a structure that is averaged over many unit cells. Even the use of local probes such as IR and Raman spectroscopy is hampered by the significant overlap of H_2O, H_3O^+, and OH bands.[31] Static ^1H NMR experiments have been used to investigate the magnetic structure and have shown that the antiferromagnetic phase is chiral. The spectrum was extremely broad below T_N, spanning more than 8 kOe (≈36 MHz) at 1.76 K.[14] The samples investigated in this study were synthesized by a conventional hydrothermal synthesis method, which has been shown to yield defect jarosite,[11] suggesting that more than one proton site is likely to be present in this material. Despite this, the powder spectrum could be fit with a model that contained one ^1H NMR site. Higher resolution NMR methods are clearly required if the different environments and their

(25) Coomer, F. C.; Harrison, A.; Oakley, G. S.; Kulda, J.; Stewart, J. R.; Stride, J. A.; Fåk, B.; Taylor, J. W.; Visser, D. *J. Phys. (Paris)* **2006**, *18*, 8847–8858.
(26) Grohol, D.; Nocera, D. G. *Chem. Mater.* **2007**, *19*, 3061.
(27) Drouet, C.; Navrotsky, A. *Geochim. Cosmochim. Acta* **2003**, *67*, 2063.
(28) Grohol, D.; Nocera, D. G. *J. Am. Chem. Soc.* **2002**, *124*, 2640.
(29) Elhajal, M.; Canals, B.; Lacroix, C. *Phys. Rev. B* **2002**, *66*, 014422.
(30) Nielsen, U. G.; Majzlan, J.; Phillips, B. L.; Ziliox, M.; Grey, C. P. *Am. Mineral.* **2007**, *92*, 587.
(31) Bishop, J. L.; Murad, E. *Am. Mineral.* **2005**, *90*, 1100.

Table 1. Chemical Composition of the Initial Solutions and Reaction Conditions as Well as Lattice Parameters Determined from Powder XRD

sample	starting composition of the synthesis solution	synthesis conditions	lattice parameters (Å)	sample composition
K-jaro	10 mL of D_2O, 0.41 g of $Fe_2(SO_4)_3$, and 0.09 g of K_2SO_4	70 °C for 1 h, 140 °C for 22 h in a 50 mL pressure bomb	$a = 7.3258(4)$, $c = 17.053(1)$	Fe = 2.4(2), K = 0.69(4), S = 2
Na-jaro	10 mL of D_2O, 0.41 g of $Fe_2(SO_4)_3$, and 0.11 g of Na_2SO_4	70 °C for 1 h, 140 °C for 22 h in a 50 mL pressure bomb	$a = 7.3395(3)$, $c = 16.7234(7)$	not determined
D_3O-jaro	10 mL of D_2O and 1.92 g of $Fe_2(SO_4)_3$	70 °C for 4 h, 155 °C for 22 h in a 50 mL pressure bomb	$a = 7.3592(2)$, $c = 16.9837(6)$	not determined
stoic-jaro	30 mL of H_2O, 20 mL of D_2O, 4.88 g of K_2SO_4, 2.2 mL (96%) of H_2SO_4, and 0.56 g of Fe	200 °C for 48 h in a 125 mL pressure bomb	$a = 7.2989(1)$, $c = 17.2271(4)$	Fe = 3.0(1), K = 0.99(3), S = 2

[a] The Fe, K and S contents for the jarosite samples were quantified using microprobe analysis. The S content was determined to be 2.00(7) and thus all Fe and K contents are normalized to S = 2.

contributions to the magnetic structure are to be elucidated. Thus, the current study focuses on the use of high resolution ^{2}H MAS NMR methods to investigate (1) the existence of the hydronium ion in jarosite, (2) the local environment near an iron vacancy, and (3) the level of ion exchange on the A site. The large hyperfine (Fermi contact) shifts seen in the spectra of these systems, due to the transfer of unpaired electron spin density from the Fe^{3+} ions to the ^{2}H nuclei, are exploited to allow the different local environments to be resolved. A detailed variable-temperature study of these samples is beyond the scope of this paper and will be reported elsewhere.[32] ^{2}H has been chosen instead of ^{1}H because (i) the ^{2}H NMR quadrupolar line shape is a sensitive probe of the deuteron motion[33–35] and (ii) the strong electron−nuclei dipolar coupling is reduced by a factor of 6.6 as compared to that of ^{1}H [$\gamma(^2H)/\gamma(^1H) = 0.15$].[36,37] Both the quadrupole and Fermi contact (hyperfine) shift interactions provide structural information concerning the strength of the hydrogen bonding and the Fe−D connectivities, respectively. Furthermore, because the ^{2}H NMR hyperfine shift region for Fe^{3+} in jarosite is ca. 270 ppm (vide infra), corresponding to ca. 60 and 9 kHz at 4.7 T for ^{1}H and ^{2}H, respectively, the potential for overlap between the isotropic resonances and the spinning side bands (ssb's) is minimized. Solid-state NMR studies of iron compounds are challenging and far from routine because of the magnetic properties of iron. Nonetheless, it has been demonstrated that high-resolution NMR spectroscopy is possible in the limit of fast electron-spin relaxation, allowing studies of iron(III) oxyhydroxides and of local environments containing paramagnetic iron centers in metal organic compounds to be performed.[36–38]

Experimental Section

Synthesis. Table 1 summarizes the chemicals and reaction conditions used to synthesize the jarosite samples investigated. A nominally stoichiometric deuterated jarosite with A = K (stoic-jaro) was prepared by the method of Grohol et al., which has been reported to yield stoichiometric samples. Iron metal was used as the iron source.[13] Three deuterated jarosite samples (A-jaro) with A = Na, K, and D_3O^+ were synthesized hydrothermally following the conventional procedure for defect jarosite samples, as previously described.[20] The reagents used were deionized water, D_2O (99.8% isotopic, Alfa-Aesar), K_2SO_4 or Na_2SO_4 (reagent grade, Fisher), and $Fe_2(SO_4)_3(H_2O)_{\sim 6.75}$ (reagent grade, Alfa-Aesar). $Fe_2(SO_4)_3(H_2O)_{\sim 6.75}$ was dehydrated before use by heating in a platinum crucible at 110 °C for 20 min, followed by 250 °C for 1 h and 500 °C for 1 h to ensure that the heat treatment did not cause loss of sulfur and the formation of iron(III) oxides (Fe_2O_3). This decomposition occurs at ~700 °C according to our thermogravimetric data. As a consequence, the ferric sulfate may not have been fully dehydrated. However, the presence of a small amount of ^{1}H in the samples does not interfere with the NMR experiments. The starting chemicals were mixed in the amounts specified in Table 1. Care was taken to ensure that all solids were dissolved in D_2O before the synthesis commenced. The clear solutions were then sealed in Teflon-lined Parr bombs and treated under the reaction conditions given in Table 1. After the hydrothermal treatment, the samples were scraped from the walls of the Teflon vessel, filtered, washed with a small amount of D_2O, and subsequently dried at 40 °C.

X-ray Diffraction (XRD). Each sample was characterized by powder XRD with a Scintag PAD V powder X-ray diffractometer, employing Cu Kα radiation and a graphite diffracted-beam monochromator.

IR Spectroscopy. IR spectra were collected in attenuated total reflectance mode, using a Bruker IFS 66 v/s Fourier transform IR spectrometer. The samples were pressed against a single-reflection diamond crystal, and the signal was detected by a DTGS detector.

Electron Microprobe Analysis. The concentrations of Na, K, Fe, and S for stoic-jaro and K-jaro were determined using a Cameca SX 100 microprobe with an accelerating voltage of 20 kV and a current of 5 μA. Because of a combination of very limited sample quantities and sample destruction by radiation, only two samples were analyzed. The instrument was calibrated using strontianite (S), hematite (Fe), and feldspars (K and Na). The results are summarized in Table 1 and have been normalized to a sulfur content, per molecular formula unit, of 2.

NMR. ^{2}H MAS NMR experiments were performed at ambient temperatures on a Chemagnetics 200 MHz spectrometer [4.7 T, $\nu_L(^2H) = 30.7$ MHz] using 4 mm HFX and 3.2 mm HX Chemagnetics probes as well as a 1.8 mm MAS probe built by Samoson et al. with 14–17 and 35–38 kHz spinning speeds, respectively. Spectra were recorded with a Hahn echo to alleviate problems with spectrometer dead time and probe ringing. In

(32) Nielsen, U. G.; Majzlan, J.; Heinmaa, I.; Samoson, A.; Grey, C. P. Unpublished results.
(33) Maricq, M. M.; Waugh, J. S. *J. Chem. Phys.* **1979**, *70*, 3300.
(34) Spiess, H. W. *Colloid Polym. Sci.* **1983**, *261*, 193.
(35) Weintraub, O.; Vega, S. *Solid State Nucl. Magn. Reson.* **1995**, *4*, 341.
(36) Cole, K. E.; Paik, Y.; Reeder, R. J.; Schoonen, M.; Grey, C. P. *J. Phys. Chem. B* **2004**, *108*, 6938.
(37) Nielsen, U. G.; Paik, Y.; Julmis, K.; Schoonen, M. A. A.; Reeder, R. J.; Grey, C. P. *J. Phys. Chem. B* **2005**, *109*, 18310.
(38) Lee, H.; Polenova, T.; Beer, R. H.; McDermott, A. E. *J. Am. Chem. Soc.* **1999**, *121*, 6884.

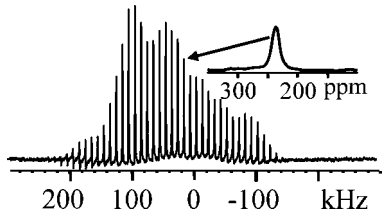

Figure 2. ^{2}H MAS NMR spectrum of stoichiometric jarosite (A = K, stoic-jaro) recorded at 55.5 MHz (8.4 T) using a spinning speed of 8 kHz.

addition, for stoic-jaro, spectra were recorded at 8.4 T [$\nu_L(^2H)$ = 55.3 MHz] using 8−10 kHz spinning. Both Hahn echo (90−180°) and single-pulse experiments were performed; the latter employed a short (5–15°) tip angle. A liquid sample of D_2O was used for referencing [$\delta_{iso}(^2H) = 4.8$ ppm] and radio-frequency calibrations. A magic-angle setting was achieved by minimizing the ssb line widths in the ^{2}H MAS NMR spectrum of deuterated sodium acetate (CD_3COONa).

Results and Discussion

Initial Characterization of the Samples by XRD and IR. The purity of the samples was verified by powder XRD, and the lattice parameters (Table 1) were calculated by a full-profile fit with the GSAS software.[39] No crystalline impurities were identified in the XRD spectra. The IR spectra suggest that the D/(D + H) ratio in the jarosite samples K-jaro, Na-jaro, and D_3O-jaro was nearly 1.00, indicating that these samples are essentially fully deuterated. In contrast, stoic-jaro (A = K) contains a mixture of OD and OH groups because the starting aqueous solution was a 3:2 mixture of H_2O and D_2O (cf. Table 1). The SO_4^{2-} stretching region (~900–1300 cm^{-1}) for our defect jarosite samples (Na-jaro, K-jaro, and D_3O-jaro) shows more than the three vibrations predicted for the C_{3v} symmetry of the sulfate group in the structure of stoichiometric jarosite, indicating that multiple local environments for sulfate must exist. However, the strong overlap of these bands and the lack of a reliable quantitative interpretation preclude the use of the bands to support our NMR data.

Stoic-Jaro (A = K). The nominal composition of a stoichiometric deuterated jarosite is $KFe_3(SO_4)_2(OD)_6$. The K and Fe concentrations found by electron microprobe analysis correspond, within the error limits of the measurement, to those expected for a stoichiometric sample (Table 1). Thus, the ^{2}H NMR spectrum should contain only one resonance. Consistent with this, a single manifold of ssb's with an isotropic resonance at $\delta = 237(4)$ ppm (Figure 2) is observed in the ^{2}H MAS NMR spectrum, where the error in the determination of the isotropic peak position was assumed to be equal to the full width at half-maximum (fwhm) of the resonance. We assign this resonance to the Fe_2OD group, the only local ^{2}H NMR environment in a stoichiometric jarosite. There are two contributions to the isotropic resonance, a small isotropic shift (ca. 4 ppm) and a large Fermi contact shift of ca. 233 ppm, the latter caused by the transfer of unpaired electron spin density originating at the Fe^{3+} ion to the s-orbital of the ^{2}H atom. The strong dipole interaction (ca. 912 ± 145 ppm, vide infra) between the ^{2}H nuclei and the unpaired d electrons on Fe^{3+} results in an asymmetric ssb manifold, which, nonetheless, bears some resemblance to the characteristic line shape (Pake doublet) for rigid OD groups. Surprisingly, for a paramagnetic material, the individual ssb's are quite narrow (a fwhm of ca. 800 Hz is observed). The size of the quadrupole interaction and the principal element of the dipole tensor were determined by using the approach of Siminovitch et al.[40] This method employs the position of the two edges of the spectrum and assumes that the axially symmetric dipole and quadrupole tensors are aligned in the same direction. The spectrum edges were assumed to be given by the position of the highest/lowest-frequency visible ssb ± half of a rotor frequency, as measured from a slow-spinning-speed ^{2}H MAS spectrum. An uncertainty in the measurement of each spectrum edge of half of a rotor period was assumed. The calculated values are summarized in Table 2. Using this approach, a quadrupolar coupling constant, C_Q, of 220(8) kHz and a dipole coupling of 912 ± 145 ppm were determined. Low-temperature ^{2}H NMR studies[32] show that this group remains rigid from 50 to 300 K. The dipolar coupling is quoted in parts per million instead of Hertz, the common unit conventionally employed for dipolar couplings, because the paramagnetic dipolar coupling scales with the magnetic field strength. The C_Q for −OD groups in oxides depends sensitively on the strength of hydrogen bonding between the deuteron and any nearby oxygen anions.[41] The measured value of 220(8) kHz is consistent with an OD−O distance of 2.79(4) Å, calculated by using correlations established by Poplett and Smith[41] between the C_Q and the D−O hydrogen-bonding distance.

D_3O-Jaro. A stoichiometric sample of deuteronium jarosite has the formula $(D_3O)Fe_3(SO_4)_2(OD)_6$. Thus, a ^{2}H MAS NMR spectrum of this compound should contain two ^{2}H NMR resonances, from Fe_2OD and D_3O^+ species, with a relative spectral intensity ratio of 2:1. In contrast, the ^{2}H MAS NMR spectrum of D_3O-Jaro (Figure 3a) shows the presence of three sets of ssb manifolds from resonances centered at $\delta \approx 0(10)$, 70 (30), and 240(60) ppm. These lines are quite broad, reflecting a distribution of Fermi contact shifts, presumably caused by the structural defects. The three resonances originate from the sample because no impurities were identified by powder XRD. Each site has a distinctive, asymmetric ssb envelope reflecting the deuteron mobility (or lack thereof) and local environment. As for stoic-jaro, the asymmetry of the ssb manifold is caused by the dipolar interaction between the ^{2}H NMR nuclei and the unpaired electron spins on Fe^{3+}. Spectra recorded with the lowest possible spinning speed (15 kHz), where none of the resonances and side bands overlap, were used for analysis. Again, the uncertainties of these measurements were estimated to correspond to a frequency of approximately half of a rotor period. This results in large errors in the determination of the dipolar couplings (500 ppm). We note

(39) Larson, A. C.; von Dreele, R. B. *General Structure Analysis System, LANSCE, MS-H805*; GSAS: Los Alamos, NM, 1994.

(40) Siminovitch, D. J.; Rance, M.; Jeffrey, K. R.; Brown, M. F. *J. Magn. Reson.* **1984**, *58*, 62.

(41) Poplett, I. J. F.; Smith, J. A. *J. Chem. Soc., Faraday Trans.* **1978**, *74*, 1077.

Table 2. ^{2}H Quadrupole Coupling Parameters and Dipole Couplings for the Different Local Environments in the Jarosite Samples Estimated Based on the Method of Siminovitch et al.[40]

sample	resonance	δ (ppm)	C_Q (kHz)[a]	η_Q	dipolar coupling (ppm)[a]	intensity[b]
stoic-jaro	Fe_2OD	237(4)	220(8)	≈0	912(260)	100
D_3O-jaro	Fe_2OD	240(60)	233(15)	≈0	1173(500)	57(33)
	$FeOD_2$	70(30)	114(15)	≈1	293(500)	14(14)
	D_nO	0(10)	98(15)		0(500)	29(2)
K-jaro	Fe_2OD	240(60)	245(15)	≈0	890(500)	63(5)
	$FeOD_2$	130(30)	99(15)	≈1	0(500)	29(4)
	D_nO	5(10)[c]	98(15)		0(500)	8(2)
Na-jaro	Fe_2OD	230(60)	227(15)	≈0	1000(500)	68(5)
	$FeOD_2$	64(30)	99(15)	≈1	98(500)	16(3)
	D_nO	1(10)	99(15)		0(500)	16(3)

[a] The uncertainty of the measurements corresponds to half of a rotor period. [b] The spectral intensities were obtained from integration of ^{2}H MAS NMR spectra recorded at 35 kHz spinning speed spectra and are normalized to 1. [c] Two partly resolved peaks at ca. 0.5 and 9.7 ppm.

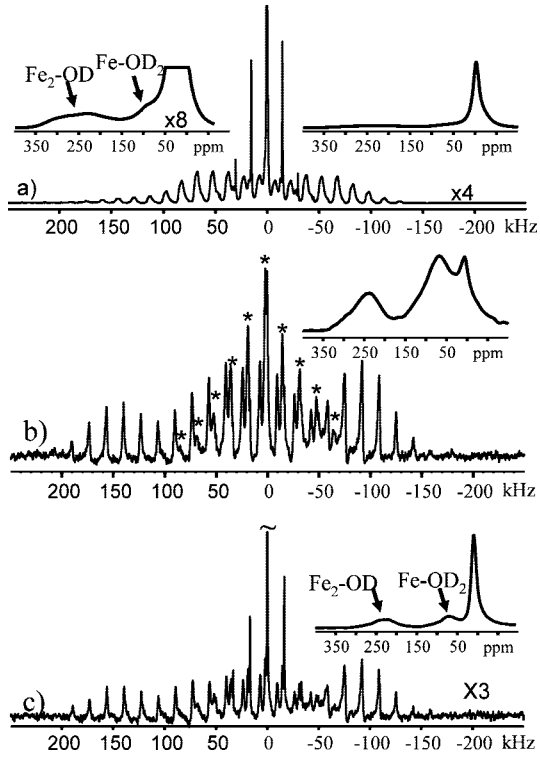

Figure 3. ^{2}H MAS NMR spectra of (a) D_3O-jaro, (b) K-jaro, and (c) Na-jaro recorded at ambient temperature using a spinning speed of 16 kHz at 30.1 MHz (4.7 T). The insets show expansions of the regions containing the isotropic resonances.

that attempts to determine the quadrupole and dipole coupling parameters by iterative fitting to the ssb intensities proved ambiguous with respect to the size of the dipolar coupling and relative orientations of the quadruple and dipole tensors. Furthermore, each site likely has a distribution of dipolar coupling parameters and local magnetic environments, due to the Fe^{3+} vacancies. Thus, each ssb pattern cannot be described by a unique set of parameters.

For the resonance at $\delta = 240(60)$ ppm, a C_Q of 233(15) kHz is obtained. These parameters are identical with those for Fe_2OD in stoic-jaro within error limits, and the overall shape of the spectrum matches that of a spectrum of stoic-jaro recorded with the same spinning speed. Thus, we assign this resonance to the Fe_2OD group. A dipolar coupling of 1170(500) ppm is obtained in good agreement with the values previously observed for iron oxyhydroxides, e.g., 600–1200 ppm for the Fe_2OD group in a deuterated goethite (α-FeOOD)[36,38] and ca. 600 ppm in lepidocrocite (β-FeOOD). Again, the observed C_Q of 230(30) kHz agrees well with the value of 225 kHz predicted using the diffraction-derived OD−O distance of 2.82 Å,[9] for the distance between the Fe−O−Fe and S−O oxygen atoms, in hydronium jarosite, and the correlation between C_Q and r_{OD-O} of Poplett and Smith.[41]

The second site with $\delta = 70(30)$ ppm, which is not observed for stoic-jaro, is associated with a C_Q of ≈114 kHz and a dipolar coupling of 300–1000 ppm. The ssb manifold is characteristic for a site with an asymmetry parameter (η_Q) ≈ 1, as is often observed for MOD_2 groups undergoing C_2 (180°) flips around the M−O bond vector.[42,43] The significant Fermi contact shift (60–70 ppm) shows that these OD_2 groups are coordinated to Fe^{3+} ions via Fe−O−D chemical bonds, and most likely only to a single iron, because the Fermi contact shift is much smaller than that for the Fe_2OD group (cf. Table 2). We therefore assign this resonance to an $FeOD_2$ group, i.e., deuterons next to an Fe^{3+} vacancy (Figure 1b).

The third ^{2}H NMR resonance with $\delta \approx 0$ ppm and $C_Q \approx$ 98 kHz is assigned to D_nO groups in cavities between the octahedral sheets, i.e., groups not directly bonded to Fe^{3+}. This isotropic shift has two contributions, an isotropic chemical shift, which is typically in the range 4–12 ppm for D_nO groups,[30,44,45] and a small hyperfine shift, whose magnitude is unknown but which appears to be small and negative in sign. It is difficult, therefore, to distinguish between D_2O and D_3O^+ based solely on the isotropic shifts. The relative intensity of the three different resonances was calculated (Table 2) by recording a 35 kHz MAS NMR spectrum where the number of ssb's was minimized, allowing the intensities of the isotropic resonances and ssb's to be summed. The average number of deuterons (n) in each A-site cavity (per D_nO oxygen) can then be calculated as follows:

$$n = 6\frac{I(D_nO)}{I(Fe_2OD) + \frac{1}{2}I(FeOD_2)} \qquad (2)$$

where $I(Fe_2OD)$, $I(FeOD_2)$, and $I(D_nO)$ are the integrated intensities of the Fe_2OD and $FeOD_2$ groups and D_nO ions, respectively, resulting in $n = 2.7(3)$ for D_3O-jaro. Thus, the majority of the A sites are occupied by deuteronium ions

(42) Soda, G.; Chiba, T. *J. Chem. Phys.* **1969**, *50*, 439.
(43) Spiess, H. W.; Sillescu, H. *J. Magn. Reson.* **1981**, *42*, 381.
(44) Bohmhammel, K.; Brand, P.; Härtig, C. *Z. Anorg. Allg. Chem.* **1986**, *542*, 201.
(45) Ripmeester, J. A.; Ratcliffe, C. I.; Dutrizac, J. E.; Jambor, J. L. *Can. Miner.* **1986**, *24*, 435.

(D_3O^+) as $n \gg 2$. Note that this result does not require any assumptions concerning the mechanism for charge compensation of the vacancy.

A general composition for a deuterated hydronium jarosite of $[(D_3O)_{1-x}(D_2O)_y]_AFe_{3-x}(SO_4)_2(OD)_{6-4x}(OD_2)_{4x}$ can then be derived by assuming (1) 100% occupancy for SO_4 and (2) that each Fe^{3+} vacancy is compensated for by reaction (1), which further requires appropriate charge compensation of the A site via the loss of a D_3O^+ ion, where "$[..]_A$" denotes the species located on the A site. The concentration of Fe^{3+} vacancies (x) can then be extracted from the intensities by using eq 3,

$$4x = 6\frac{\frac{1}{2}I(FeOD_2)}{I(Fe_2OD) + \frac{1}{2}I(FeOD_2)} \quad (3)$$

yielding a value of $x = 0.16(3)$ for D_3O-jaro. On the basis of this concentration of Fe^{3+} vacancies and reaction (1), only 0.84(3) D_3O^+ ions may be present on the A site, resulting in a value for the small occupancy of the A site by D_2O molecules, y, of only 0.09(20). Thus, a total occupancy of 0.94(20) for the A site and a sample composition of $[(D_3O)_{0.84(3)}(D_2O)_{0.09(20)}]_AFe_{2.84(3)}(SO_4)_2(OD)_{5.4(1)}(OD_2)_{0.6(1)}$ are derived based on NMR.

The A site occupancy is in good agreement with the value (0.91) obtained from single-crystal XRD for a hydronium jarosite sample prepared by one of us in an identical fashion to that used to prepare D_3O-jaro.[20] This observation of a very high concentration of D_3O^+ ions is consistent with the observation of hydronium ions in near-stoichiometric alunite samples.[30,44,45] Finally, it should be noted that the relative intensities of the different resonances are not consistent with the protonation of the Fe−O(D)−Fe linkages by D_3O^+ ions: this mechanism would imply a much higher concentration of $FeOD_2$ groups than was seen experimentally via NMR.

K-Jaro. The ideal composition of a stoichiometric deuterated jarosite is $KFe_3(SO_4)_2(OD)_6$, yet the ^2H MAS NMR spectra of K-jaro contain the same three resonances as those observed for D_3O-jaro albeit with quite different relative intensities (Figure 3b). The D_3O^+/D_2O peak is weak and accounts for less than 10% of the total spectral intensity. In contrast, the $FeOD_2$ intensity is larger and about half that of the Fe_2OD intensity. A value of $x = 0.29(5)$, corresponding to ca. 10% Fe^{3+} vacancies, can be obtained from eq 3 and the values given in Table 2. Thus, the number of Fe^{3+} vacancies is larger than that in D_3O-jaro. This is in agreement with the general observation that hydronium or deuteronium jarosite usually contains fewer Fe^{3+} site vacancies when prepared using the conventional synthesis procedure.[12] The ^2H quadrupole coupling parameters and isotropic shifts (Table 2) are identical with those obtained for D_3O-jaro, in agreement with the invariance of the local environment of the Kagomé layer to cation substitution.[1]

The general composition of a defect jarosite is $[K_{1-x-z}(D_3O)_z(D_2O)_y]_AFe_{3-x}(SO_4)_2(OD)_{6-4x}(OD_2)_{4x}$, again assuming that either a deuteronium ion is deprotonated or a K^+ ion is absent for each Fe^{3+} vacancy (eq 1). Only one resonance is observed in the D_nO region, whose asymmetric line shape suggests the presence of two overlapping resonances with $\delta \approx 9.7$ and 0.5 ppm and thus the presence of both D_2O and D_3O^+. On the basis of the intensity of this resonance, a value for the total D(n) content on the A site of 0.62(16) is obtained. Assuming that D_2O molecules predominate, then the total D_2O occupancy is limited by the A site occupancy, which cannot exceed 1, yielding a composition $[K_{0.70(9)}(D_3O)_{0.01(8)}(D_2O)_{0.30(8))}]_AFe_{2.7(1)}(SO_4)_2(OD)_{4.8(2)}(OD_2)_{1.2(2)}$, with very few or no D_3O^+ ions (model 1). Conversely, if all of the deuterons are present as D_3O^+ ions, then the D_3O^+ content is constrained by the need for the charge balance imposed by eq 1, yielding a formula $[K_{0.50(8)}(D_3O)_{0.21(6)}]_AFe_{2.7(1)}(SO_4)_2(OD)_{4.8(2)}(OD_2)_{1.2(2)}$ (model 2). The predicted K^+ content is then lower than the values of 0.7–0.9 typically reported for jarosite.[13,27] Microprobe analysis yields an occupancy of 0.69(4) for K on the A site (Table 1), indicating that the nature of the water species present on the A site is closer to that predicted by model 1; i.e., water molecules predominate.

The presence of water is fully consistent with the charge compensation mechanism proposed in eq 1. If, however, we now assume that this mechanism is *not* operative in jarosite and that an Fe^{3+} vacancy is only compensated for by three H^+ ions, then eq 3 is no longer appropriate. 33% more Fe^+ vacancies must be present than was calculated above from the intensity of the $FeOD_2$ resonance, i.e., $x = 0.4(1)$. Equation 2 is independent of the charge compensation mechanism, and thus the number of deuterons on the A site, n, remains unchanged. Now, charge balance of the negatively charged framework requires that the A site is fully occupied with monovalent cations (K^+ and/or H_3O^+), yielding the formula $[K_{0.8}(D_3O)_{0.2}]_AFe_{2.6(1)}(SO_4)_2(OD)_{4.8(2)}(OD_2)_{1.2(2)}$. The K^+ content is larger than that observed experimentally (even including the large errors associated with the elemental analysis), providing additional evidence for the charge compensation mechanism given in eq 1.

Na-Jaro. The nominal composition of a stoichiometric deuterated natrojarosite is $NaFe_3(SO_4)_2(OH)_6$. The ^2H MAS NMR spectrum of this sample (Figure 3c) shows that this sample is also nonstoichiometric but with fewer $FeOD_2$ groups (i.e., Fe^{3+} vacancies) as compared to K-jaro. The integrated intensities of the $FeOD_2$ and D_2O/D_3O^+ peaks are of comparable magnitude (Table 2), showing a substantial ion exchange of Na^+ for D_2O/D_3O^+ in this defect natrojarosite, with the D_2O/D_3O^+ concentration being noticeably higher than that in K-jaro. Values of $x = 0.16(4)$ and $n = 1.26(25)$ can be calculated from eqs 3 and 2, respectively. Because only one D_3O^+ is destroyed per four $FeOD_2$ groups created and $x = 0.16(4)$ (eq 1), a significant amount of D_3O^+ must be present on the A site. Again, if we assume that all of the D_nO signal originates from D_3O^+ (model 2), the formula $[Na_{0.42(9)}(D_3O)_{0.42(8)}]_AFe_{2.85(5)}(SO_4)_2(OD)_{5.4(2)}(OD_2)_{0.6(2)}$ is obtained. Conversely, assuming that all $1 - x$ sites are filled by D_2O (model 1), i.e., the A site is fully occupied, a formula $[Na_{0.53(9)}(D_3O)_{0.31(8)}(D_2O)_{0.16(4)}]_AFe_{2.85(5)}(SO_4)_2(OD)_{5.4(2)}(OD_2)_{0.6(2)}$ is obtained. In both cases, the A site contains a substantial amount of D_3O^+ ions and more than that seen in K-jaro. We note that the Na occupancy obtained with both assumptions is smaller than is generally (0.7−0.9) observed for natroalunite samples.[27] It is possible that a hydrous

diamagnetic impurity phase may be present, such as an amorphous sodium sulfate. However, no crystalline impurities were detected in powder XRD.

Interpretation of the Hyperfine Shifts

The isotropic shifts determined for the Fe_2OD and $FeOD_2$ groups in paramagnetic jarosite are much larger than the shifts of 4−11 ppm that have been observed in the isostructural diamagnetic alunite samples.[30,44,45] The hyperfine interaction is given by

$$H = A\langle S_z \rangle \tag{4}$$

for systems where the electron spin relaxation is fast on the NMR time scale, where A is the hyperfine constant and $\langle S_z \rangle$ the time-averaged value of the electronic spin (in the direction of the static magnetic field), defined as follows:

$$\langle S_z \rangle = -\frac{B_0}{\mu_0 g N_0 \mu_B}\chi_M \tag{5}$$

B_0 is the magnetic field, μ_0 permeability, g the electron g factor, N_0 Avogadro's number, μ_B the Bohr magneton, and χ_M the magnetic susceptibility. For spin-only magnetism, the magnetic susceptibility is given by the spin-only formula ($\chi_M = (S(S+1))^{1/2}\mu_B$). The hyperfine interactions result in a hyperfine (Fermi contact) shift by transfer of an unpaired electron spin density from Fe^{3+} to the ^2H nucleus via the different molecular (or crystal) orbitals. This mechanism is analogous to the *J*-coupling interaction between two nuclear spins. Hyperfine shifts are excellent probes of the local magnetic environment because the size and sign of these shifts may often be estimated by analysis of shifts in related model compounds and by application of the Goodenough−Kanamori rules to rationalize these shifts. For example, the sizes of the $^{6,7}Li$ hyperfine shifts have been correlated with the Li local environments and d-electron configurations, leading to the construction of a paramagnetic shift scale for lithium manganese oxides[46,47] and for identification of inner-sphere complexes on iron oxyhydroxide surfaces.[37,48] Fe^{3+} has a $3d^5$ (high-spin) configuration in jarosite with half-filled d orbitals. The deuterium atom in the Fe_2OD group is located slightly (ca. 9°) above the plane defined by the Fe−O(2)−Fe bonds, the *xy* plane in Figure 4a,b; thus, there are interactions with both the O p_x and p_z orbitals and indirectly with the half-filled d_{xz} (or d_{yz}) orbital (Figure 4a) and with the d_{xy} orbital (Figure 4b). On the basis of the geometry, the interaction with the d_{xy} orbital is predicted to be the strongest. The two Fe−O−D bond angles in the Fe_2OD group are identical (ca. 112°);[20] thus, one Fe−O−D bond results in a hyperfine shift of ≈115 ppm.

Stoichiometric jarosite samples have an effective magnetic moment close to the value predicted for Fe^{3+} high-spin ions from the spin-only formula (5.92 μ_B),[13] but values higher than this (6.4−7.29 μ_B) are reported for nonstoichiometric jarosite.[9,11,20,49] The narrow (800 Hz) line shapes observed for stoic-jaro (Figure 2) show the presence of a single, well-defined local magnetic environment in agreement with the crystal structure. For the samples containing vacancies (D_3O-jaro, K-jaro, and Na-jaro), a large distribution of hyperfine shifts (ca. ±50 ppm) are observed for both Fe_2OD and $FeOD_2$, reflecting significant variation in the *local* chemical and magnetic environment due to iron vacancies. This distribution is centered at the position (within the error limit) of the isotropic resonance in stoic-jaro (Table 2).

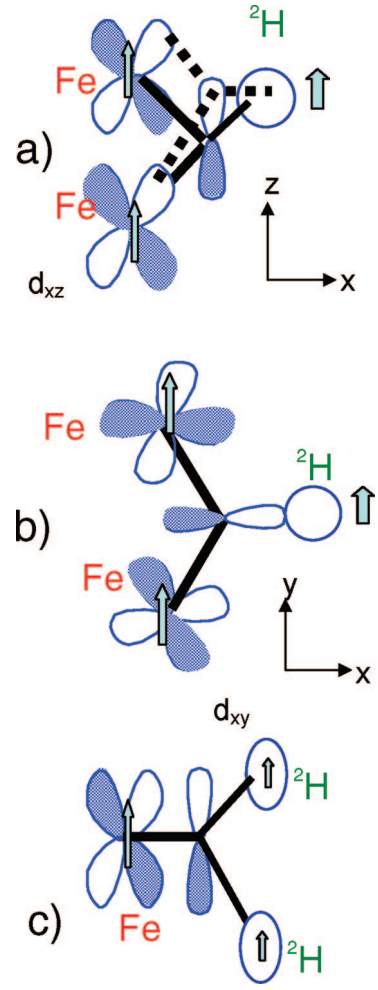

Figure 4. Magnetization transfer pathways for the deuteron species for Fe_2OD via the (a) d_{xz} (d_{yz}) and (b) d_{xy} orbitals and (c) for the $FeOD_2$ group near a vacancy via d_{xz} (d_{yz}) orbitals.

To a first approximation, a shift of approximately 115 ppm is expected for the $FeOD_2$ group near an iron vacancy (Figure 1) because each OD_2 group is coordinated to a single Fe^{3+} ion. This is much larger than the experimentally observed value (70 ppm; cf. Table 2), which is ascribed to differences in the bond angles and distances between those for the $FeOD_2$ and Fe_2OD groups. Figure 4c illustrates a possible magnetization transfer pathway for this group. Deuterons in $FeOD_2$ groups are more acidic than those in Fe−O(D)−Fe groups based on simple charge-balance arguments. For example, partial charges of Fe_2O^- and $FeO(H)^{0.5-}$ can be estimated for the two oxygen atoms using the MUSIC model, which

(46) Grey, C. P.; Dupre, N. *Chem. Rev.* **2004**, *104*, 4493.
(47) Grey, C. P.; Lee, Y. J. *Solid State Sci.* **2003**, *5*, 883.
(48) Kim, J.; Nielsen, U. G.; Grey, C. P. *J. Am. Chem. Soc.,* accepted.
(49) Earle, S. A.; Ramirez, A. P.; Cava, R. J. *Physica B* **1999**, *262*, 199.
(50) Hiemstra, T.; van Riemsdijk, W. H. *J. Colloid Interface Sci.* **1996**, *179*, 488.
(51) Hiemstra, T.; Venema, P.; Riemsdijk, W. H. V. *J. Colloid Interface Sci.* **1996**, *184*, 680.
(52) Venema, P.; Hiemstra, T.; Weidler, P. G.; van Riemsdijk, W. H. *J. Colloid Interface Sci.* **1998**, *198*, 282.

assigns charges based on the number and charges of the coordinated atoms.[50–52] Thus, a proton coordinated to Fe_2O^- will form a much stronger bond with a shorter O−H bond length than a proton coordinated to $Fe-O(H)^{0.5-}$, resulting in a larger hyperfine shift per Fe−O−D bond for a deuteron in a Fe_2OD group rather than in a $FeOD_2$ group.

Based on the small ^2H quadrupole coupling constant, the hydronium ion and water molecules on the A site are highly mobile at room temperature. Indeed, Ripmeester et al. could simulate their experimental ^2H static NMR line shapes for the D_nO groups in their deuterated hydronium alunite by using a 12-site jump model involving hydrogen bonding to the six $Al_2O(H)$ and six oxygen atoms at the base of the sulfate tetrahedron.[45] A small negative shift is observed herein these species, suggesting that transfer of the spin density only occurs via weaker hydrogen bonds. As discussed above, hydrogen bonding involving either the oxygen or proton of the Fe−O(H)−Fe linkage to the H_2O/H_3O^+ species will not be strong because the partial charge on the oxygen atom on the Fe−O(H)−Fe linkage is close to zero and the Fe−O(H)−Fe O−H bond is strong.

Grohol et al. have ascribed the absence of magnetic long-range order and resultant spin-glass behavior at low temperature in hydronium jarosite to the disorder created by both an intrinsic proton-transfer reaction, $H_3O^+ + Fe_2OH \rightarrow H_2O + Fe_2OH_2$, and an extrinsic reaction, i.e., the consumption of H_3O^+ by defects.[13] Additional disorder (or lowering of the space group symmetry) will also exist because of the multiple sites for the H_3O^+ ions in the cavities,[9,20] which could also affect long-range magnetic ordering. In a more recent paper,[26] these authors presented additional IR data for a (K and H_3O) jarosite solid-solution series and again suggested, based on this data and the strongly exothermic nature of the reaction $OH^-(aq) + H_3O^+(aq) \rightarrow 2H_2O(l)$ in aqueous solutions, that protonation of the Fe_2OH groups occurs.[26] Our ^2H NMR results do not provide any compelling evidence for this reaction. In addition, spin-counting data suggest that the majority of the A site is occupied by D_3O^+ ions in D_3O-jaro. Furthermore, simple formal charge calculations predict that the oxygen atoms in the Fe−O(H)−Fe linkage are not basic and are thus expected to be chemically inert. Thus, we suggest that the spin-glass behavior is more likely associated with the disorder due to the multiple positions for H_3O^+ within the A-site cavities.

Conclusions

New insight into the local structure and dynamics of defect jarosite samples has been obtained by using solid-state ^2H MAS NMR spectroscopy. The samples investigated here have different compositions, ranging from stoichiometric (stoic-jaro) to defect (Na-jaro and K-jaro) phases with about 5–9% Fe^{3+} vacancies. Three different local environments, Fe_2-OD, Fe-OD_2, and D_2O/D_3O^+, were identified based on their Fermi contact shifts and ^2H quadrupole couplings, allowing the concentration of vacancies and the extent of cation exchange in the A site of the jarosite structure to be quantified. The ^2H MAS NMR spectra indicate that substantial exchange (Na^+/K^+ for D_3O^+/D_2O) on the A site occurs, with a K^+ occupancy in K-jaro of only 70% and a Na^+ occupancy of 40–50% in Na-Jaro. The hydronium ion is unambiguously identified in D_3O-jaro, confirming that this ion remains intact in stoichiometric regions of the samples, as was previously observed for alunite.[30] The NMR spectra for K-jaro are consistent with a charged Fe^{3+} vacancy charge-compensated for by four H^+ ions, providing an explanation for the presence of H_2O on the A site and the partial occupancy of this site seen in some jarosite samples. We find no evidence for the reaction $Fe_2OH + H_3O^+ \rightarrow Fe_2OH_2 + H_2O$, indicating that this reaction is not the cause of the absence of long-range magnetic order in hydronium jarosite.[13]

The paramagnetism of the samples results in improved spectral resolution over that observed for isostructural diamagnetic samples: the resonances are distributed over ca. 250 ppm, in contrast to the less than 10 ppm chemical shift range observed in diamagnetic alunite.[30] Thus, the Fe−O(D)−Fe and $FeOD_2$ groups and the D_nO groups on the A site are readily separated, with the Fermi contact shifts for these groups representing finger prints of the Fe−O−D connectivities. The Fe_2OD groups are rigid, and an OD−O distance of 2.79(4) Å is obtained from an analysis of the ^2H MAS NMR spectra, in excellent agreement with the crystal structure. The $FeOD_2$ groups undergo rapid C_2 flips around the Fe−O bond axis, while the hydronium ion is highly mobile.

In conclusion, this study illustrates that solid-state NMR spectroscopy can provide detailed information concerning the local environments of proton-containing defects in paramagnetic materials. This information can sometimes represent the critical missing data required to connect structure with physical properties such as magnetism or to understand mechanisms for the incorporation of dopant ions into the structure and the formation of metastable phases, particularly in samples prepared via aqueous-based routes. These data are often extremely difficult to obtain via other techniques.

Acknowledgment. U.G.N. acknowledges the "Camille and Henry Dreyfus Postdoctoral Program in Environmental Chemistry" and Carlsbergfondet (Grant ANS-1323/20) for financial support. J.M. appreciates support from the Hess postdoctoral fellowship at the Department of Geosciences at Princeton University. The Center for Environmental Molecular Science is sponsored by the NSF (Grant CHE-0221934).

Supporting Information Available: Complete refs 5 and 7. This material is available free of charge via the Internet at http://pubs.acs.org.

CM702523D